Blucher Mechanical Engineering Proceedings
May 2014, vol. 1 , num. 1
www.proceedings.blucher.com.br/evento/10wccm

10th World Congress on Computational Mechanics
8-13 July 2012 • São Paulo • Brazil

NUMERICAL INVESTIGATION OF PARTICLE MOTION IN SUPERSONIC FLOWS

R. Sakamaki[1], M. Suzuki[2], and M. Yamamoto[3]

[1]Graduate School of Mechanical Engineering, Tokyo University of Science

[2]Clean Engine Team, Aviation Program Group, Japan Aerospace Exploration Agency

[3]Department of Mechanical Engineering, Tokyo University of Science
(yamamoto@rs.kagu.tus.ac.jp)

Abstract. *Gas-particle two-phase flow is very important to clarify phenomena inside of various fluid machines. A number of reserches have been performed on gas-particle two-phase flows. However, particle motion in a supersonic flow has not been clarified sufficiently. Therefore, in order to find out the interactions between flow and particles, the authors focus on the characteristics of particle motion, especially the velocity and temperature. In the present study, a conventional converging-diverging supersonic nozzle is employed as our target. For the gas phase, the turbulent flow in the nozzle is computed with the finite difference and RANS methods. For the particle phase, the particle motion is simulated in a Lagrangian manner. In addition, taking into account the light particle loading, a weak coupling method is employed. Through this investigation, we show that the particle velocity increases monotonically from the nozzle throat to the outlet. And it is shown that particles can be accelerated to higher velocities in helium than in nitrogen, and smaller particles tend to attain higher speed and lower static temperature.*

Keywords: *Gas-solid two-phase flow, Supersonic flow, Euler-Lagrange coupling*

1. INTRODUCTION

Gas-particle two-phase flows have attracted a great deal of attention in the fields of science, engineering, and medicine. A great deal of theoretical, experimental, and numerical research has been reported. For example, Kliegel [1] investigated the flow in a supersonic nozzle of a solid-fueled rocket. He derived the one-dimensional governing equations for the two-phase flow inside the nozzle, and successfully verified these equations through comparison with corresponding experimental data. Shi [2] researched the interaction process concerning many complicated non-linear aerodynamic relationships, which is the interactons between vortices in the wakes of particle and the dynamic shock wave such as reflection, diffraction, and focusing. However, it is too difficult to clarify the phenomenon precisely. Saito et al. [3]

investigated unsteady drag on particles by shock wave, to discuss an interaction between shock wave induced flow and a solid particle affects the flow structure that is obtained with a steady drag force. Ishii et al. [4] performed computations for a gas-particle two-phase flow around a sphere in order to mimic the flow around the blunt nose of a supersonic vehicle. Investigating the computational results, they clarified the characteristic differences between the single-phase flow and the gas-particle two-phase flow. They found that a large particle cloud can distort the shock-layer around a sphere. Recently, Liu [5] numerically and experimentally investigated a miniature supersonic nozzle designed for use in a drug delivery system. In his system, helium (He) was selected as the carrier gas, and the flow was accelerated to a Mach number of 4. As mentioned above, a number of studies on gas-particle two-phase flow can easily be found in the literatures. However, the behavior of particles in a supersonic flow has not been clarified satisfactorily. Therefore, the particle behavior in a supersonic flow should be clarified in order to design various machines using gas-particle two-phase flows.

In the present study, we focus on the particle temperature in supersonic flows, in order to clarify the interaction between fluid and particles. The turbulent flow in a nozzle was computed with the finite difference and RANS methods, and the particle motion was simulated in a Lagrangian manner. In addition, taking into account the light particle loading, we employed a weak coupling method. The numerical results of the particle velocity and temperature reasonably agree with the experimental data.

2. NUMERICAL PROCEDURES

2.1. Algorithm

The computational procedures for the two-phase flow are as follows:

Step 1. Compute the turbulent flow field

Step 2. Compute the particle trajectory

Since the particle concentration in the flow field is small enough to ignore particle-particle collisions and interactions with the flow field from the particle-phase, that is, one-way coupling is adopted. According to Elgobashi [6], when the volumetric particle concentration is less than 10^{-6}, these assumptions are justified. Detailed methodologies of each step are described below.

2.2. Gas phase

In the present study, numerical simulations are conducted using a finite difference technique. The gas-phase is considered to be a continuous phase, while the particle-phase is a dispersed one. As mentioned above, the particle-phase has no influence on the gas-phase. Therefore, the gas-phase flow can be computed in the same manner as for the single-phase flow. The gas-phase flow is assumed to be compressible, turbulent and axi-symmetric. It is calculated using the Eulerian approach, based on the Favre-averaged continuity, Navier-Stokes and energy equations (i.e., RANS approach). The governing equations can be given by

$$\frac{\partial \bar{\rho}}{\partial t} + \frac{\partial}{\partial x_j}\left(\bar{\rho}\tilde{u}_j\right) = 0 \tag{1}$$

$$\frac{\partial}{\partial t}\left(\bar{\rho}\tilde{u}_i\right) + \frac{\partial}{\partial x_j}\left\{\bar{\rho}\tilde{u}_i\tilde{u}_j + \bar{p}\delta_{ij} - \left(\bar{\tau}_{ij} - \overline{\rho u_i'' u_j''}\right)\right\} = 0 \tag{2}$$

$$\frac{\partial}{\partial t}\left(\bar{\rho}\tilde{e}_t\right) + \frac{\partial}{\partial x_j}\left\{\left(\bar{\rho}\tilde{e}_t + \bar{p}\right)\tilde{u}_j - \left(\bar{\tau}_{ij}\tilde{u}_i - \bar{q}_j - \overline{\rho e_t'' u_j''}\right)\right\} = 0 \tag{3}$$

where x_i are the Cartesian coordinates, u_i, q_j and τ_{ij} are the velocity, heat flux and viscous stress tensor; t, ρ, p and e_t denote the time, density, static pressure and total energy of the fluid, respectively, (−), (~) and (") indicate the Reynolds averaging operation, the Favre averaging operation and the fluctuating component of Favre average, respectively. For the turbulence model, the standard k-ε model proposed by Launder and Spalding [7] is introduced.

The governing equations are discretized using the second-order upwind TVD scheme [8] for the inviscid terms, the second-order central difference scheme for the viscous terms, and the four-stage Runge-Kutta method [9] for the time integration. The local time stepping method is used in order to reduce the computational time required to obtain the steady sate solutions.

2.3 Particle phase

The particle phase is treated using a Lagurangian approach, in which particles are tracked in time along their trajectories through the flow field. The present study is conducted under the following assumptions:

- ✓ Particle is spherical and non-rotating
- ✓ Particle-to-particle collision is neglected
- ✓ The particle phase has no influence on the gas phase
- ✓ The only force acting on a particle is drag

Under these assumptions, the equation of the particle velocity and temperature are described using velocity and temperature of the gas phase,

$$\frac{du_{pi}}{dt} = \frac{3C_D\rho_g}{4\rho_p D_p}\left(u_{gi} - u_{pi}\right)\left|V_{rel}\right| \tag{4}$$

$$\frac{dT_p}{dt} = \frac{6h}{C_p\rho_p D_p}\left(T_g - T_p\right) \tag{5}$$

$$V_{rel} = \sqrt{\left(u_{gj} - u_{pj}\right)^2} \tag{6}$$

where subscripts g and p denote the gas and particle phase, and D_p and C_p are the diameter and specific heat of a particle. The drag coefficient C_D is defined by calculating the relative Reynolds number based on the relative velocity between the gas-phase and the particle as follows:

$$C_D = \begin{cases} \dfrac{24}{\mathrm{Re}_p}\left(1 + 0.15\,\mathrm{Re}_p^{\,0.687}\right) & (\mathrm{Re}_p < 1000) \\ 0.4 & (\mathrm{Re}_p \geq 1000) \end{cases} \tag{7}$$

$$\mathrm{Re}_p = \frac{D_p \left| u_{gi} - u_{pi} \right|}{\nu} \tag{8}$$

where ν is kinematic viscosity of the gas-phase. The coefficient of heat transfer h can be expressed as:

$$h = \frac{\lambda Nu}{D_p} \tag{9}$$

$$\mathrm{Nu} = 2 + 0.6\,\mathrm{Pr}^{1/3}\,\mathrm{Re}_p^{\,1/2} \tag{10}$$

where λ, Pr, and Nu are the heat conductivity, Prandtl number, and Nusselt number. Finally the particle trajectory is calculated by integrating the following equation in time with the first-order Euler explicit method.

$$\frac{dx_{pi}}{dt} = u_{pi} \tag{11}$$

Note that, in the present study, we ignore the turbulence effects of gas phase on particles. This is based on the follow consideration. Since the flow in the nozzle is highly accelerated with a strongly favourable pressure gradient, the favourable pressure gradient suppresses turbulence (and in some case relaminarization takes places).

3. COMPUTATIONAL CONDITION

3.1 Computational domain and grid

In the present study, the computational domain is an axi-symmetric convergent-divergent nozzle. The schematic view is shown in Figure 1. In the figure, l_1 and l_2 are the length between the nozzle inlet and the nozzle throat, and between the nozzle throat and the nozzle outlet. A_{in}, A_{th} and A_{out} denote the nozzle inlet diameter, nozzle throat diameter, and nozzle outlet diameter, respectively.

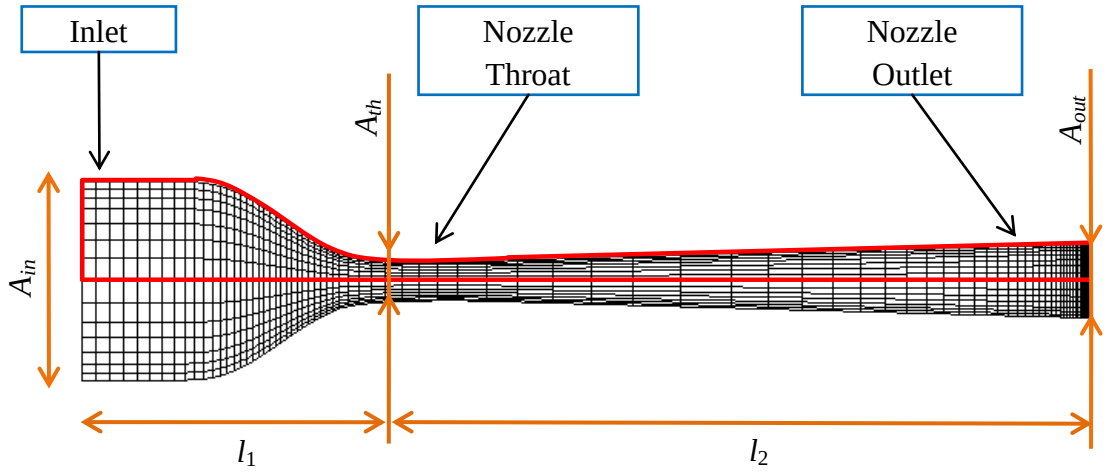

Figure 1 Computational domain and grid

The total grid number is 101 × 51 inside the nozzle, as shown in Figure 1. This grid number is sufficient because we employ the high-Reynolds number k-ε model with a wall function.

3.2 Computational conditions

The computational conditions in the present study are as follows. Two working fluids, i.e., helium (He) and nitrogen (N_2) are simulated. The Prandtl number is assumed to be 0.71 in N_2 case and to be 0.68 in He case. The turbulent Prandtl number is set 0.9 in both cases. Three inlet static temperatures, 873.15, 1073.15, and 1273.15[K] are employed, to clarify the effect of inlet static temperature. At the inlet boundary, the static temperature and the mass flow rate are fixed by assuming isentropic condition, and the density is extrapolated. The nozzle walls are assumed to be of no-slip and adiabatic.

3.3 Particle

In the present study, we assume the particle material to be titanium. The density is 4510 [kg/m^3] and the specific heat is 520 [J/kgK]. In order to investigate the effect of particle diameter, a number of trials are conducted while varying the particle diameter: 1.0, 5.0, 10.0, 20.0, 60.0, 80.0 and 100.0 [μm]. One particle is released from the center of the inlet of the computational domain at same velocity and temperature as the incoming gas.

4. RESULT AND DISCUSSION

4.1 Gas Phase

The velocity and static temperature distributions along the nozzle axes are compared with the experimental results measured by Fukanuma [10], as shown in Figures 2 and 3. These figures are obtained for the case of working gas of N_2 and the inlet temperature of

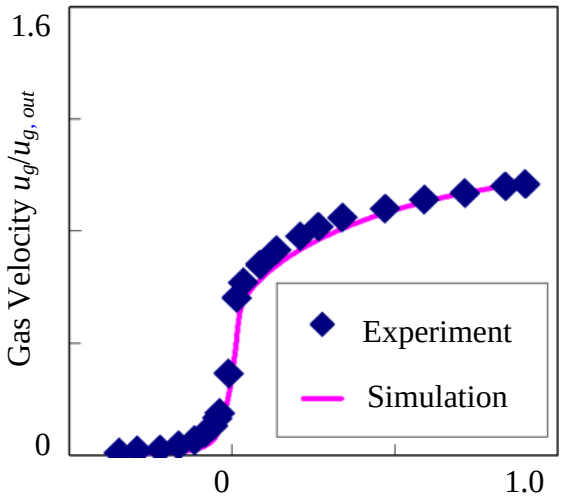

Figure 2 Axial Velocity along Nozzle Center

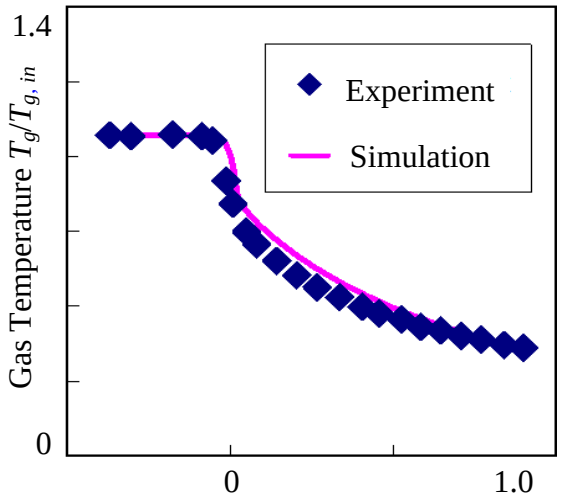

Figure 3 Gas Temperature along Nozzle

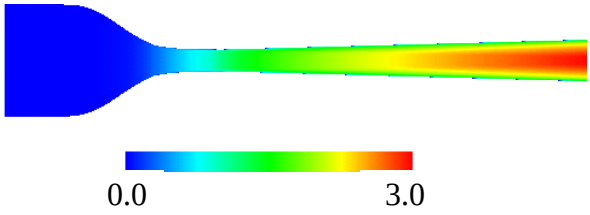

Figure 4 Mach Number in N_2 Case

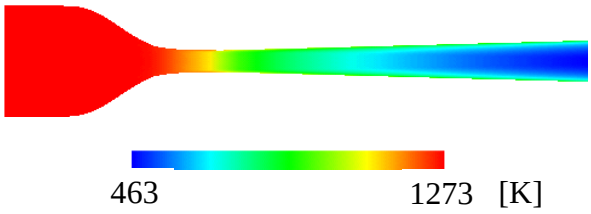

Figure 5 Static Temperature in N_2 Case

1273.15[K]. The numerical results show that the velocity of the gas phase quickly increases around the nozzle throat, and then gradually increases from the nozzle throat to the nozzle outlet. Meanwhile, the static temperature of the gas phase decreases sharply around the nozzle throat, and gradually diminishes from the nozzle throat to the nozzle outlet. Apparently, the numerical results of the gas phase are in good agreement with the trend of experimental results. The average error is about 5%, and so the present numerical simulations are fairly validated.

The distributions of Mach number and static temperature in N_2 case are respectively illustrated in Figures 4 and 5. These figures are obtained for the case of inlet temperature of 1273.15[K]. From the figures, it is clearly observed that Mach number monotonously increases from the nozzle throat (approximately 1) to the nozzle outlet (approximately 3). Static temperature shows the exactly opposite to the Mach number distribution. It is confirmed that these distributions would affect both particle velocity and temperature. Note that the results of He case indicate the similar tendency as mentioned above. These findings come into line with Jen et al. [11].

4.2 Particle phase

Figures 6 and 7 are the velocity and temperature histories of a particle, comparing the computational results with the experiments. The particle velocity is in good agreement with the experimental data, whose average error is less than 4%. On the other hand, apparently, the particle temperature is underestimated from the nozzle inlet to the nozzle throat. This mis-

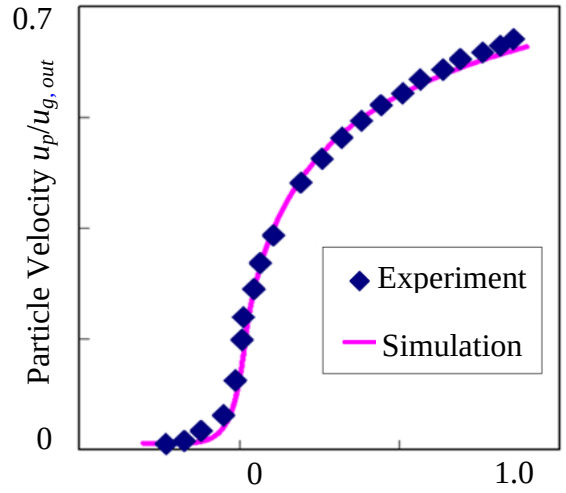

Figure 6 Particle Velocity

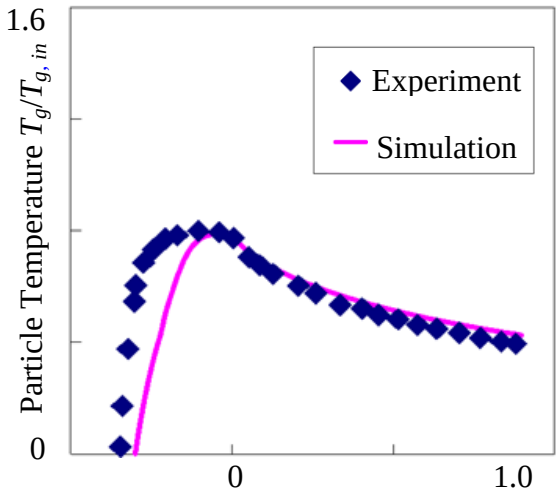

Figure 7 Particle Temperature

match may be caused from the difference of the inlet particle temperatures between the numerical and the experimental conditions. However, from the nozzle throat to the nozzle outlet, particle temperature is in good agreement with the experimental data, because the small particle is easily heated.

Histories of particle velocity and temperature are shown in Figures 8 and 9. In both figures, (a) and (b) correspond to the working gas of He and N_2, respectively. These figures are obtained from the case of inlet temperature of 1073.15[K]. Furthermore, the results are plotted for the different particle diameters: 1.0, 10.0, 20.0, 60.0, 80.0 and 100.0[μm]. Note that the vertical axes are normalized by the maximum velocity for the He case in Figure 8. The particle velocity monotonously increases from the nozzle throat to the nozzle outlet. Comparing these cases, we can confirm that using He as a working gas can accelerate a particle faster than when using N_2 as a working gas, due to the higher Mach number in the nozzle. In addition, as the particle diameter increases, the particle velocity decreases. Figure 9 shows that the

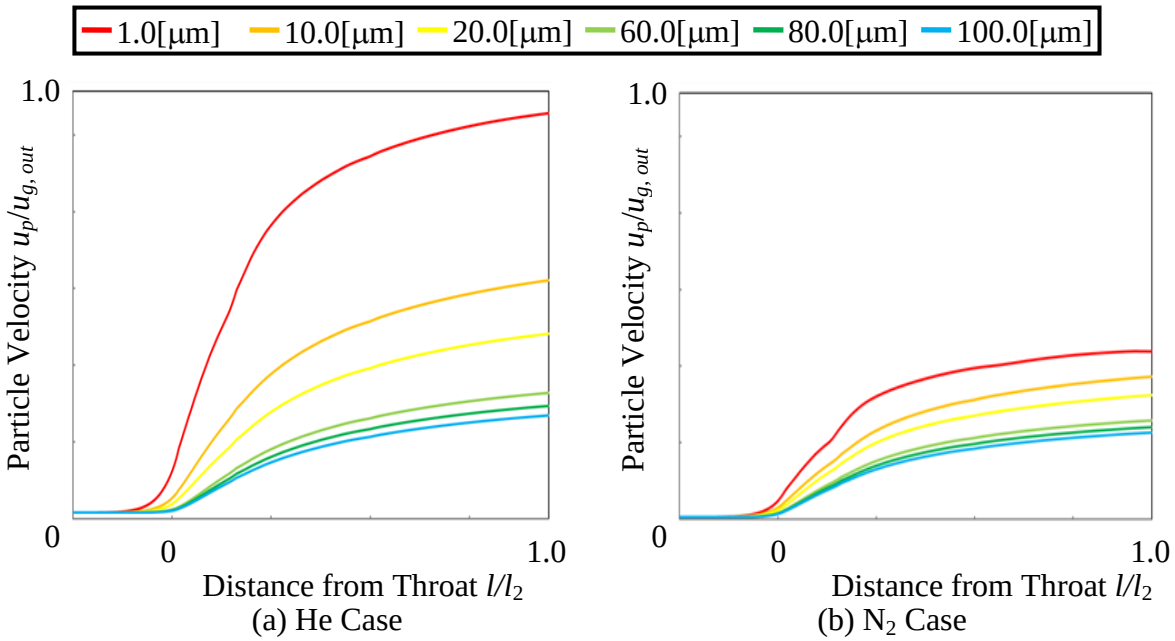

(a) He Case (b) N_2 Case

Figure 8 Particle Velocity History

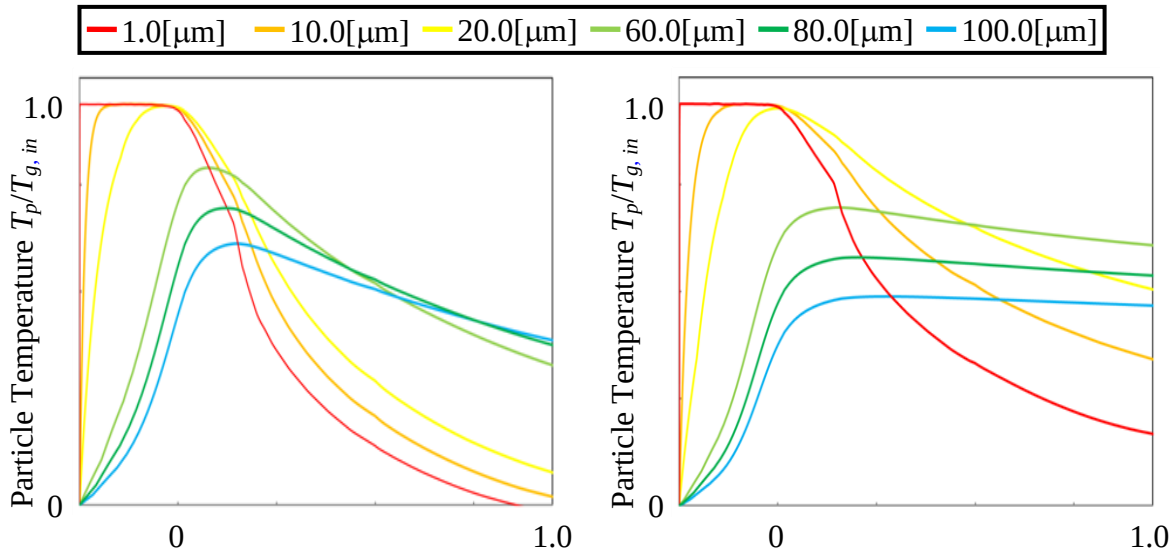

Figure 9 Particle Temperature History

particle temperature has a peak around the nozzle throat. The particle temperature of the N_2 case is generally higher than that of the He case. Smaller particles are more likely to be affected by the working gas conditions, i.e., as the particle diameter increases, the peak temperature decreases.

Figure 10 exhibits the velocity and temperature histories of a particle with the particle diameter of 20.0 [μm]. In this paragraph, the influence of the inlet gas temperature is discussed. Figure 10(a) shows particle velocity, and Figure 10(b) shows particle temperature. Note that the vertical axes of Figure 10 indicate the particle velocity normalized by the maximum velocity in the He and 1273.15 [K] case and the particle temperature normalized by the inlet gas temperature of 1273.15 [K], respectively. The particle velocity is influenced only slightly by the inlet temperature. Comparing three inlet temperature cases, the particle veloci-

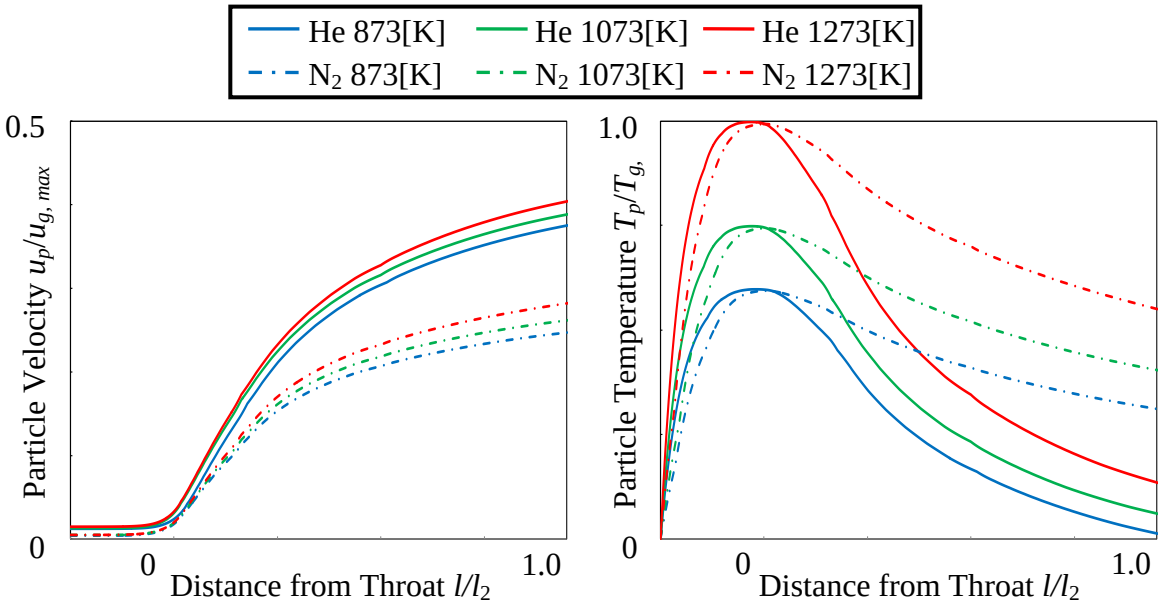

Figure 10 Particle Temperature Histories Comparing Gas Phase Conditions

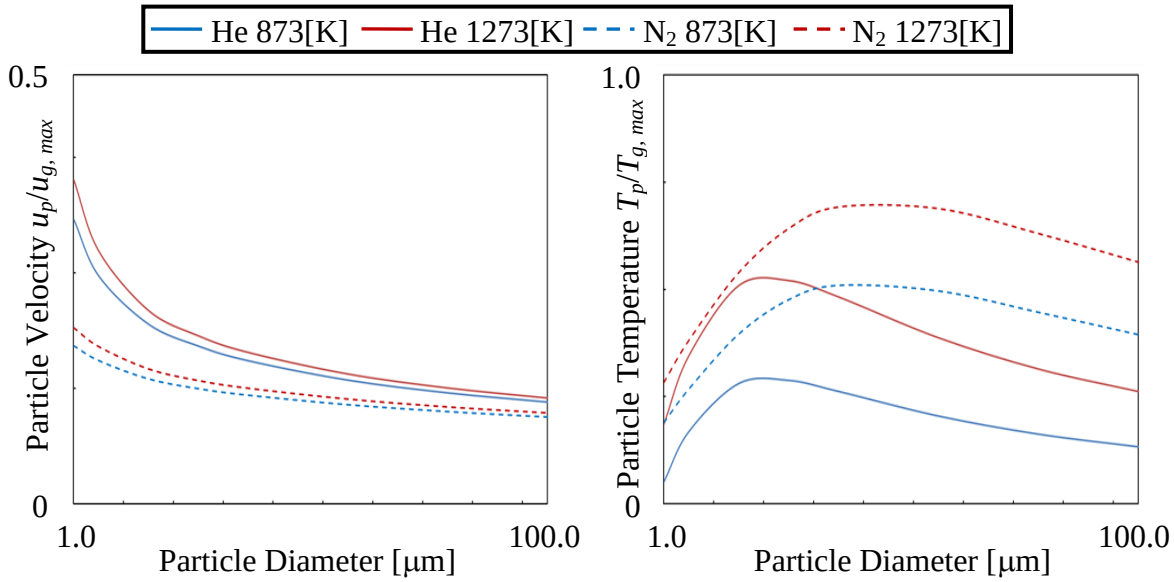

(a) Particle Velocity (b) Particle Temperature

Figure 11 Relation Between Particle Diameter and Particle Condition at Nozzle Outlet

ty in the case of 1273.15 [K] is the fastest. For both working gases, the velocity difference among three inlet temperature cases becomes larger as the nozzle outlet is approached. The particle temperature in the He case is lower at the nozzle outlet. Moreover, the temperature difference for three cases is larger at the nozzle throat than that at the nozzle outlet. In terms of the particle temperature history in both working gas cases, the change along the nozzle axis exhibits a similar trend.

Figure 11 shows the particle velocity and particle temperature at the nozzle outlet with particle diameter of 1.0 to 100.0 [μm]. In this paragraph, when the inlet temperature and the gases are changed, the status of the particle coming out from the nozzle, i.e., the particle velocity and the particle temperature are discussed. Note that the vertical axes of Figure 11 indicate the particle velocity normalized by the maximum velocity in the He and 1273.15 [K] case and the particle temperature normalized by the inlet gas temperature of 1273.15 [K], respectively. From Figure 11(a), same as Figure 8, as the particle diameter increases, the particle velocity decreases. It is worth noting that the gradients of the particle velocity for the change in the particle diameters are different. In the event of between the smaller particles, the magnitude of the gradient will be bigger, in turn, between the bigger particles have less value. This is due to assumption of the force acting on a particle, that is, the particle velocity is proportional to the projected area. From Figure 11(b), it notably turns out that a particle in each gas condition has a peak temperature of a particle diameter. Adding to that, the N_2 case is able to heat a particle more than the He case, and the peak temperature for the He case is smaller than that for the N_2 case.

5. CONCLUSION

In the present study, to clarify the gas-solid two-phase flow inside a supersonic nozzle, 2 step calculations were conducted, based on the one-way coupling. The numerical procedure

consisted of the computations of the gas flow field and solid particle trajectory. Parametric simulations were performed, with changing three inlet temperatures of 873.15 to 1273.15[K], particle diameter of 1.0 to 100.0[μm] and working fluids of He and N_2. The results drawn from this investigation are summarized below:

- The particle velocity increases monotonically from the nozzle throat to the nozzle outlet, and the particle temperature has a peak around the nozzle throat.
- As the particle diameter increases, the particle velocity and the peak temperature decrease.
- The particle velocity with a working gas for the He can accelerate a particle faster than working gas for the N_2. The particle temperature for the He case is generally lower than that of N_2 case. Smaller particles are apt to be affected by working gas conditions.
- Inlet static temperature of gas phase is of great effect to the particle temperature, despite of relatively less effect to the particle velocity.
- Smaller particle are accelerated more than larger particle, and a particle in each gas condition has a peak temperature.

6. REFERENCES

[1] Kleigel, J. R. , "Gas Particle Nozzle Flows", *Symposium on Combustion*, 9, 1, 811-826, 1963

[2] Shi, H. H., Yamamura, K., "The interaction between shock waves and solid spheres arrays in a shock tube", *Acta Mechanica Sinica*, 20(3), 219-227, 2004

[3] Saito, T., Saba, M., Sun, M., Takayama, K., "The effect of an unsteady drag force on the structure of a non-equilibrum region behind a shock wave in a gas-particle mixture", *Shock Waves*, 17, 255-262, 2007

[4] Ishii, R., Hatta, N., Umeda, Y. and Yuhi, M., "Supersonic Gas-Particle two-Phase Flow around a Sphere", *J. Fluid Mechanics,* 221, 453-483, 1990

[5] Liu, Y. , "The Use of Miniature Supersonic Nozzles for Microparticle Acceleration: A Numerical Study", *IEEE Transactions on Biomedical Engineering*, 54, 10, 1814-1821, 2007

[6] Elghovashi S., "On Pedicting Particle Laden Turbulent Flows", *Applied Science Research*, 52, 309-329, 1994

[7] Launder B. E., Spalding D. B., "THE NUMERICAL COMPUTATION OF TURBULENT FLOWS", *Computational Meth. Appl. Mech. Eng.* 3, 2, 269-289, 1974

[8] Yee H. C., "Upwind and Symmetric Shock Capturing Schemas", *NASA-TM-89469*, 1987

[9] Jameson A. and Baker T. J., “Solution of the Euler Equations for Complex Configurations”, *AIAA-83-1929*, 293-302, 1983

[10] Hirotaka F., “The development of High Temperature and Pressure Cold Spray Equipment”, *Japan Thermal Spray Society*, 47, 179-188, 2010

[11] Jen T.C., Li L., Cui W., Chen Q. Zhang X., “Numerical Investigations on Cold Gas Dynamic Spray Process with Nano- and Microsize Particles”, *Int. J. Heat Mass Tran*., 12, 48, 4384-4396, 2005